View metadata, citation and similar papers at core.ac.uk
brought to you by CORE
provided by Elsevier - Publisher Connector

Neuron 51, 687–697, September 21, 2006 ©2006 Elsevier Inc. DOI 10.1016/j.neuron.2006.08.023

# The Prototoxin *lynx1* Acts on Nicotinic Acetylcholine Receptors to Balance Neuronal Activity and Survival In Vivo

**Julie M. Miwa,[1,2] Tanya R. Stevens,[1,2] Sarah L. King,[2,6] Barbara J. Caldarone,[2] Ines Ibanez-Tallon,[1,7] Cheng Xiao,[5] Reiko Maki Fitzsimonds,[3,8] Constantine Pavlides,[4] Henry A. Lester,[5] Marina R. Picciotto,[2] and Nathaniel Heintz[1,*]**

[1] The Laboratory of Molecular Biology
Howard Hughes Medical Institute
The Rockefeller University
New York, New York 10021

[2] Department of Psychiatry
Yale University School of Medicine
New Haven, Connecticut 06510

[3] Department of Cellular and Molecular Physiology
Yale University School of Medicine
New Haven, Connecticut 06510

[4] Department of Neuroendocrinology
The Rockefeller University
New York, New York 10021

[5] Division of Biology
California Institute of Technology
Pasadena, California 91125

## Summary

**Nicotinic acetylcholine receptors (nAChRs) affect a wide array of biological processes, including learning and memory, attention, and addiction. *lynx1*, the founding member of a family of mammalian prototoxins, modulates nAChR function in vitro by altering agonist sensitivity and desensitization kinetics. Here we demonstrate, through the generation of *lynx1* null mutant mice, that lynx1 modulates nAChR signaling in vivo. Its loss decreases the $EC_{50}$ for nicotine by ~10-fold, decreases receptor desensitization, elevates intracellular calcium levels in response to nicotine, and enhances synaptic efficacy. *lynx1* null mutant mice exhibit enhanced performance in specific tests of learning and memory. Consistent with reports that mutations resulting in hyperactivation of nAChRs can lead to neurodegeneration, aging *lynx1* null mutant mice exhibit a vacuolating degeneration that is exacerbated by nicotine and ameliorated by null mutations in nAChRs. We conclude that lynx1 functions as an allosteric modulator of nAChR function in vivo, balancing neuronal activity and survival in the CNS.**

## Introduction

Nicotinic acetylcholine receptors (nAChRs) make up a family of ionotropic, ligand-gated ion channels, which contribute to a wide range of functions in the central nervous system, including learning and memory, locomotion, and attention (reviewed in Rezvani and Levin, 2001; Picciotto et al., 2000). nAChRs are gated by the neurotransmitter (NT) acetylcholine (ACh), which is released from axonal terminals distributed throughout the brain, as well as by the drug nicotine, which is the primary addictive agent in tobacco (US Department of Health and Human Services, 1988). Activation of postsynaptic nAChRs induces depolarizing inward currents that typically increase firing frequencies, whereas activation of nAChRs located on presynaptic terminals contributes to $Ca^{2+}$ flux into the terminal augmenting NT release (reviewed in Dani, 2001). Activation of nAChRs can thus shift the balance of competing inhibitory and excitatory inputs toward excitation, producing synaptic changes that can facilitate learning and memory (Mann and Greenfield, 2003, Mansvelder and McGehee, 2000).

The importance of maintaining the proper balance of cholinergic signaling has been well documented. For example, reductions in nAChR levels or activity have been correlated with Alzheimer's disease, schizophrenia, Parkinson's disease, and dementia (Picciotto and Zoli, 2002; Lindstrom, 1997), and mice lacking nAChR subunits exhibit enhanced neurodegeneration (Zoli et al., 1999). Under some circumstances, nAChR activation can play a neuroprotective role, reducing the cell's sensitivity to excitotoxicity, while in other cases, overactivation of nAChRs can be detrimental. For instance, high doses of nicotine can induce epilepsy (Damaj et al., 1999) and cause cell death (Abrous et al., 2002), and knockin mice with hyperactive α7 or α4 nAChRs exhibit lower seizure thresholds (Fonck et al., 2003, 2005; Broide et al., 2002) and suffer from neuronal loss (Orb et al., 2004; Labarca et al., 2001; Orr-Urtreger et al., 2000). Even subtle alterations in nAChR activity, such as those resulting from changes in desensitization kinetics, can have important consequences on cholinergic function (Dani et al., 2000; Wooltorton et al., 2003). One form of epilepsy, ADNFLE, caused by mutations in the widely expressed nAChR subunits α4 or β2, results from altered desensitization and gating properties of nAChRs (Bertrand et al., 1998; Kuryatov, et al., 1997). Taken together, these studies highlight the importance of cholinergic tone in normal CNS function and illustrate the detrimental effects that chronic hyperactivation of nAChRs can have on neurons and neuronal ensembles in vivo.

We have previously reported the identification of a cholinergic modulator, lynx1 (Miwa et al., 1999), which can form stable associations with nAChRs and alter their function in vitro (Ibanez-Tallon et al., 2002). *lynx1*, an evolutionary precursor to snake venom toxins, shares structural characteristics with toxins such as α- and κ-bungarotoxins, which bind tightly to nAChRs and inhibit their activation. When coexpressed with lynx1, α4β2 nAChRs are less sensitive to ACh, display more rapid desensitization, and recover more slowly from desensitization. Single-channel studies of α4β2 receptors indicate that lynx1 shifts the distribution of channel

*Correspondence: heintz@mail.rockefeller.edu
[6] Present address: Department of Psychology, University of Sussex, Brighton BN1 9QG, United Kingdom.
[7] Present address: Max-Dulbrick Center for Molecular Medicine, Rovert-Rossle-Strasse 10, Berlin, 13125 Germany.
[8] Present address: Yale University, P.O. Box 7611, New Haven, Connecticut 06519.

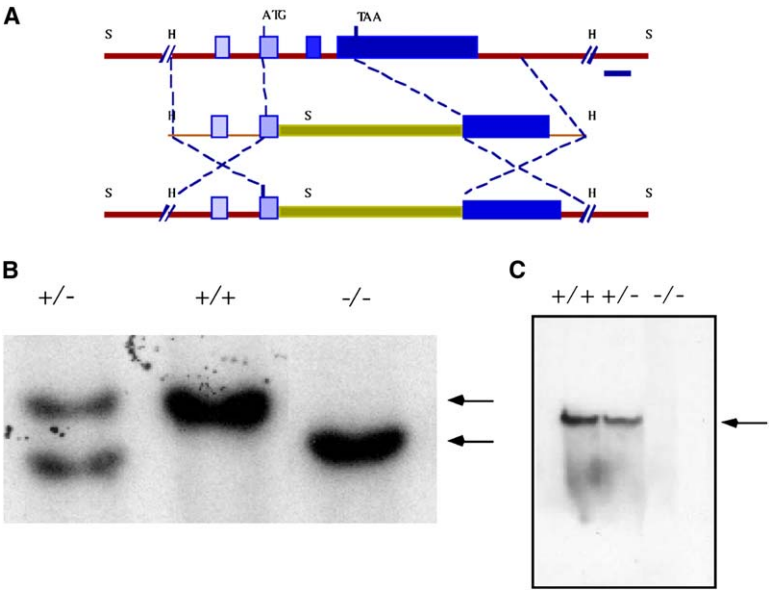


Figure 1. Generation of *lynx1* Null Mutations through Targeted Mutagenesis

(A) Targeting strategy to remove the *lynx1* gene using homologous recombination. The upper diagram represents a large region of genomic DNA surrounding the *lynx1* gene, including its four exons (blue boxes) spanning 6 kb. The targeting construct (middle) represents a 9 kb HindIII (H) lynx1 genomic fragment, with the *neo* gene (green) inserted after the second exon of the *lynx1* gene. The bottom part of the drawing represents the modified *lynx1* gene after recombination.

(B) Genomic Southern analysis of *lynx1* null mutant mouse genomic DNA demonstrates loss of the *lynx1* coding sequence. The mutant SSP1 band is 12 kb (upper arrow), and the wt band is 9 kb (lower arrow).

(C) Western blot analysis demonstrates a loss of the lynx1 protein in *lynx1*$^{-/-}$ brain extracts.

openings toward a faster inactivating species with more uniform, larger amplitude currents. These data, along with studies showing that lynx1 colocalizes and coimmunoprecipitates with $\alpha$7 and $\beta$2 nAChR subunits, are strong indicators that lynx1 has a critical role in modulating cholinergic activity in vivo.

To test the hypothesis that lynx1 serves as an endogenous regulator of nAChR activity in vivo, we generated a targeted deletion of the *lynx1* gene in mice using homologous recombination. Because lynx1 both decreases nAChR sensitivity and increases desensitization, we postulated that its removal would reduce nAChR desensitization and increase ligand sensitivity, a condition that could lead to novel insights into cholinergic function. We report here that neurons from *lynx1* null mutant brains demonstrate heightened sensitivity to nicotine, and a corresponding increase in $Ca^{2+}$ levels in response to nicotine treatment. In addition, *lynx1* null mutant animals display enhanced learning and memory in a fear-conditioning paradigm and show a correlated reduction in paired-pulse facilitation (PPF). They also display an increased sensitivity to nicotine in the rotarod test of motor learning. These data support the hypotheses that lynx1 normally decreases activity of nAChRs and, thus, deletion of *lynx1* shifts the balance in favor of increased neuronal activity and synaptic plasticity.

Our studies also reveal that the short-term benefits of the loss of lynx1 are counterbalanced by an increased vulnerability of *lynx1* mutant neurons to glutamate toxicity and by loss of nicotine's neuroprotective effect on these cells. Consistent with these findings, *lynx1* mutant mice exhibit age-dependent degeneration that is exacerbated by nicotine and rescued by null mutations in nAChR subunits. These data are consistent with previous studies demonstrating the neurotoxic effects of mutant hypersensitive variants of nAChRs in vivo. Taken together, our data demonstrate that lynx1 modulates nAChR function in vivo and that it plays a critical role in maintaining a balance between the beneficial effects of short-term nAChR activation and the potentially devastating degenerative effects of chronic activation of these critical CNS receptors.

## Results

### Generation of *lynx1* Null Mutant Mice

We generated a deletion of the *lynx1* coding sequence through gene targeting in mice using homologous recombination in ES cells (Figure 1A). The targeting construct was designed to replace the entire lynx1 coding sequence. Homologous recombination was detected by Southern blot analysis (Figure 1B). As expected, the complete loss of lynx1 protein in the *lynx1*$^{-/-}$ animals was evident in Western blots of protein extracts from *lynx1*$^{-/-}$ relative to wild-type$^{+/+}$ and *lynx1*$^{+/-}$ littermate brains (Figure 1C). The *lynx1*$^{-/-}$ animals demonstrated no gross abnormalities in size, viability, CNS morphology, or longevity (data not shown).

### Nicotine-Induced Currents in *lynx1* Null Mutant Mice Demonstrate Hypersensitivity to Agonist

Direct measurements of nicotine sensitivity were carried out using whole-cell patch-clamp recordings of neurons in brain slices of *lynx1*$^{-/-}$ versus wild-type mice. The medial habenula was chosen for these experiments because of the high level of expression of nAChRs (Sheffield et al., 2000) and the coexpression of lynx1 and nAChRs in this region. Application of a 250 ms nicotine pulse to neurons in the medial habenula (Figure 2B) elicited larger peak responses in slices from *lynx1*$^{-/-}$ animals than those of wild-type animals (Figure 2A) for nicotine concentrations between 1 and 20 $\mu$M. For the entire tested nicotine concentration range (0.1 $\mu$M to 300 $\mu$M), the data reveal a decrease in the $EC_{50}$ from 89.0 $\pm$ 2.2 $\mu$M in wild-type mice to 9.0 $\pm$ 0.7 $\mu$M in *lynx1*$^{-/-}$ mice (Figure 2C). These currents were blocked by the nAChR antagonist mecamylamine (mec) and recovered during wash out (middle traces), indicating a specific involvement of nAChRs in this response. Analysis of the decay rate of the nicotine response revealed that the half-maximal response times in neurons from

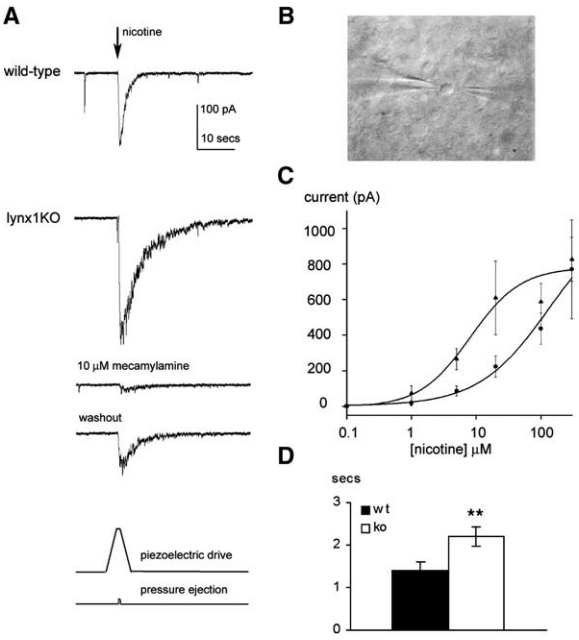


Figure 2. Hypersensitive Nicotinic Responses in the Medial Habenula of *lynx1* Null Mutant Mice

Whole-cell patch-clamp recordings from neurons in wt versus *lynx1* null mutant brain slices. (A) Representative recordings from a habenular neuron in response to nicotine. The top traces show a response to 20 μM nicotine, of a wt neuron (upper) and a *lynx1*$^{-/-}$ neuron (lower), followed by its response during perfusion of 10 μM mec and a wash out of at least 5 min. The bottom traces show the command to the piezoelectric manipulator (penultimate), which places the pipette tip within 20 μm of the cell, and to the pressure apparatus (bottom), which ejects a 250 ms pulse of nicotine.

(B) Micrograph of a *lynx1*$^{-/-}$ habenular neuron, with recording pipette (left) and nicotine-filled application pipette (right).

(C) Average whole-cell responses from neurons in slices from wt or *lynx1*$^{-/-}$ mice in response to nicotine at concentrations ranging from 0.1 μM to 300 μM. t test, $p < 0.01$ at 5 μM. 0.1 μM, n = 3 (ko), 3 (wt); 1 μM, n = 3 (ko), 3 (wt); 5 μM, n = 18 (ko), 8 (wt); 20 μM, n = 5 (ko), 4 (wt); 100 μM, n = 5 (ko), 6 (wt); 300 μM, n = 2 (ko), 5 (wt). $EC_{50}$ is 89.0 ± 2.2 with a nH = 1.3 (wt) and 9.0 ± 0.7 μM, nH = 1.1 (ko).

(D) Significant increase in the time to decay to 50% of the maximal response to 5 μM nicotine. 1.40 ± 0.19 s in wt (n = 8) and 2.20 ± 0.22 s in *lynx1*$^{-/-}$ (n = 16) neurons. t test, $p < 0.01$.

Error bars show mean ± SEM.

*lynx1*$^{-/-}$ mice (2.2 ± 0.22 s) were significantly prolonged compared to those of wild-type neurons, (1.4 ± 0.19 s) (Figure 2D). The peak responses are determined primarily by activation processes and show clear hypersensitivity, and these kinetic data also suggest that removal of lynx1 can alter the deactivation and/or desensitization processes of nAChRs in vivo.

### *lynx1* Null Mutant Neurons Display Increased Sensitivity to Nicotine

Since some aspects of nicotinic receptor hypersensitivity may be mediated via intracellular $Ca^{2+}$ levels, we measured the effect of nicotine on $Ca^{2+}$ levels in primary cortical cultures from *lynx1*$^{-/-}$ and wild-type mice. Neurons were exposed either to buffer or 10 μM nicotine. Cultured cells were then loaded with the $Ca^{2+}$-sensitive indicator fluo-3, and fluorescence measurements were obtained (Figure 3A). Incubation of wild-type cultures with 10 μM nicotine did not result in a significant change in steady-state $Ca^{2+}$ levels, whereas *lynx1*$^{-/-}$ cultures demonstrated a 2-fold increase in fluorescence (Figure 3B). These data indicate an effect of lynx1 on ligand sensitivity and/or desensitization of nAChRs.

In order to test agonist sensitivity further, we measured acute responses to nicotine by measuring fluorescence levels in real time. Nicotine elicited a significant increase in $Ca^{2+}$ levels in *lynx1*$^{-/-}$ but not in wild-type cultures (Figure 3C). Dose-response measurements indicate that ~1 μM nicotine is sufficient for activation of nAChRs and elevation of $Ca^{2+}$ levels in *lynx1*$^{-/-}$ cultures (Figure 3D), but under our conditions, no change in fluorescence was observed at any of the concentrations tested for wild-type cultures (Figure 3D). We conclude that the altered response properties of nAChRs in *lynx1* mutant cells can result in elevated intracellular $Ca^{2+}$ levels, perhaps leading to changes in intracellular signaling.

### Removal of *lynx1* Alters Synaptic Activity

Maintenance of intracellular $Ca^{2+}$ homeostasis is critical for neuronal excitability and synaptic activity. Given the enhanced sensitivity of neurons from *lynx1* null mutant mice to nicotine and the elevations in $Ca^{2+}$ levels observed in these cells in response to nicotine, it seemed likely that changes in synaptic NT release would be present in *lynx1* null mutant mice. Since synaptic responses are sensitive to nicotine in the hippocampus and both lynx1 (Miwa et al., 1999) and nAChRs are present in this brain region (Maggi et al., 2004), we tested whether excitatory synaptic responses were altered in *lynx1*$^{-/-}$ hippocampal slices. We conducted field potential recordings of evoked CA3 to CA1 synaptic responses and measured PPF ratios, an indicator of the probability of NT release, by applying two consecutive stimuli at intervals ranging from 10 to 70 ms. As expected, potentiation of the second response relative to the first response was observed at latency intervals of 30–70 ms in wild-type slices (Figure 4A), as residual $Ca^{2+}$ from the first stimulus adds to the $Ca^{2+}$ influx during the second, leading to more vesicle fusion and a potentiation of NT release. In contrast, PPF ratios in *lynx1*$^{-/-}$ slices were significantly reduced relative to wild-type responses at intervals of 50–70 ms (Figures 4A and 4B). Previous studies have suggested that a reduction in PPF reflects an increased probability of vesicle fusion and NT release, leading to a depletion of vesicle pools available to respond to subsequent stimuli. These data suggest alterations in synaptic efficacy in *lynx1*$^{-/-}$ mice.

### Enhanced Associative Learning in *lynx1* Null Mutant Mice

nAChR activation has been shown to be an important component of specific aspects of learning and memory (Picciotto et al., 1995). Therefore, a series of behavioral tests were run on *lynx1* null mutant animals to evaluate learning and memory abilities relative to their wild-type littermates. Mice were trained in a fear-conditioning paradigm, a test of associative and contextual learning. On the training day, an unconditioned stimulus of a mild foot shock was paired with a conditioned stimulus, an innocuous tone. When mice were placed into the identical training environment 24 hr later, *lynx1*$^{-/-}$ mice and

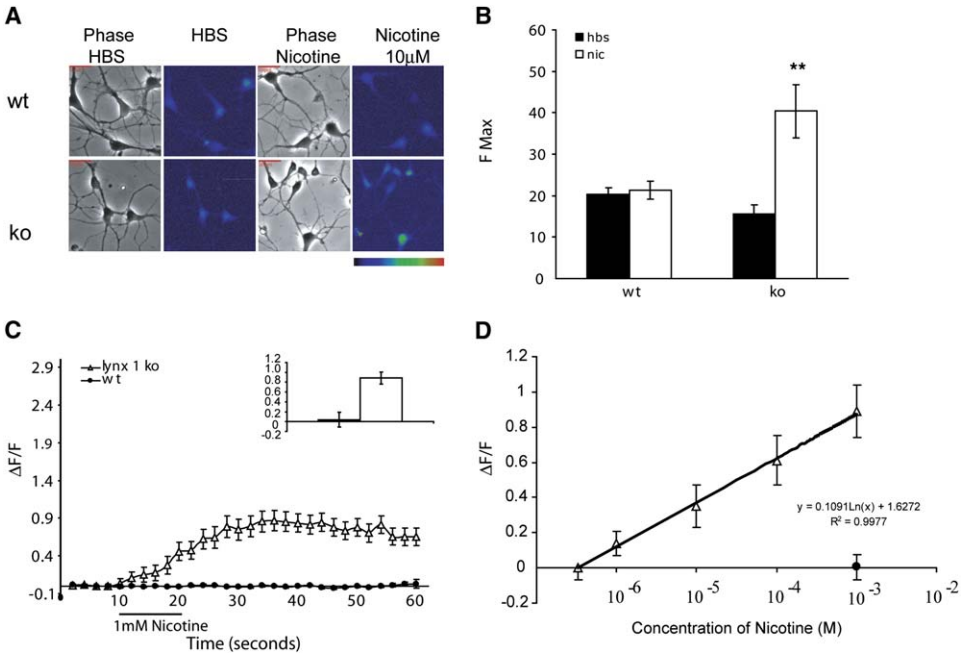


Figure 3. Elevated $Ca^{2+}$ Levels in Response to Nicotine in Primary Cortical Cultures of *lynx1* Null Mutant Mice

(A) Chronic treatment of 10 μM nicotine (1 hr) increased basal levels of fluorescence in *lynx1*$^{-/-}$ cultures. Wild-type cultures demonstrated no difference in fluorescence between buffer (HBS)-treated and nicotine-treated cultures (upper panels). *lynx1*$^{-/-}$ cultures, however, demonstrated an increase in baseline fluorescence upon nicotine treatment (lower panel, right two micrographs) as compared to HBS (lower panels, left two micrographs). Corresponding phase contrast pictures are to the left of each fluorescence image. Scale bar, 50 μm.

(B) *lynx1*$^{-/-}$ neuronal cultures display elevated $Ca^{2+}$ levels in cultures pretreated with 10 μM nicotine. Complete data collected from (A) also indicated no significant difference in fluorescence levels in wt cultures treated with HBS (black) versus nicotine (white). Data represent at least 40 cells per genotype and condition. Student t test, p = 0.0007.

(C) *lynx1*$^{-/-}$ neurons show increased $Ca^{2+}$ levels with acute applications of 1 mM nicotine. Images of the fluo-3-loaded cells were obtained for 50 s at 2 s intervals. 1 mM nicotine (horizontal bar) was applied for 10 s. Cultures from wt mice show no significant changes in fluorescence in response to nicotine, whereas the *lynx1*$^{-/-}$ cultures exhibit a significant increase in intracellular $Ca^{2+}$. The inset panel represents the maximal fluorescence level obtained upon nicotine exposure for each cell as a fraction of baseline values. These studies were conducted in at least three different cultures. Student's t test, p = 0.038; *lynx1*$^{-/-}$, n = 18 cells; wt, n = 24 cells.

(D) Dose-response relation for intracellular $Ca^{2+}$ levels in response to varying nicotine concentrations (1 μM to 1 mM, 10 s application). The *lynx1*$^{-/-}$ cultures exhibit an increase in intracellular $Ca^{2+}$ with increasing concentration of nicotine. In wt cultures, there is no change in fluorescence at the highest dose (1 mM nicotine). These studies were conducted in at least three cultures. *lynx1*$^{-/-}$ cultures: 1 mM, n = 32 cells; 0.1 mM, n = 20 cells; 10 μM, n = 32 cells; and 1 μM, n = 28 cells. Wild-type cultures, n = 24 cells, mean ± SEM.

Error bars show mean ± SEM.

wild-type littermates showed no difference in their freezing response, demonstrating that *lynx1*$^{-/-}$ mice are normal with respect to contextual learning (Figure 5A, left). In cue-associated learning, the animals were placed into a novel environment and presented with the shock-associated tone. *lynx1*$^{-/-}$ mice demonstrated a significant increase in freezing to tone as compared to their wild-type littermates, indicating an alteration in associative learning (Figure 5A, right). The animals did not show differences when placed in the altered environment, prior to the presentation of tone, indicating no difference in unconditioned fear (data not shown). These data are suggestive of a specific effect of lynx1 on associative fear learning as compared to either unconditioned fear or contextual memory.

To assess the specificity of action of lynx1 in memory processes, *lynx1*$^{-/-}$ mice were analyzed in two other forms of contextual conditioning: passive avoidance conditioning and Morris water maze learning. In passive avoidance conditioning, mice were placed in the light chamber of a two-chambered box, and the latency to enter into the dark, preferred chamber was measured, whereupon the mice were given a mild foot shock. *Lynx1*$^{-/-}$ display no differences from wild-type when the latency to enter into the dark chamber was measured the following day (Figure 5B). Mice were then assessed for performance in the Morris water maze learning task. Mice were trained for 8 days to swim through water to reach a stationary hidden platform, and the latency to find the platform was measured. No significant differences were observed between *lynx1*$^{-/-}$ and wild-type mice (Figure 5C) in either the training phase (left) or when the hidden platform was relocated to a different position on the ninth day (the transfer test, upper right). These data are consistent with the lack of effect observed in *lynx1* null mutant mice in the contextual component of the fear-conditioning task.

These behavioral data are suggestive of a specific involvement of lynx1 in cue-associated learning as opposed to contextual memory. Alternatively, enhanced freezing to tone in *lynx1*$^{-/-}$ mice could be due to a generalized increase in fear, although the lack of difference in baseline freezing or freezing to context argues against this. To test for differences in anxiety levels,

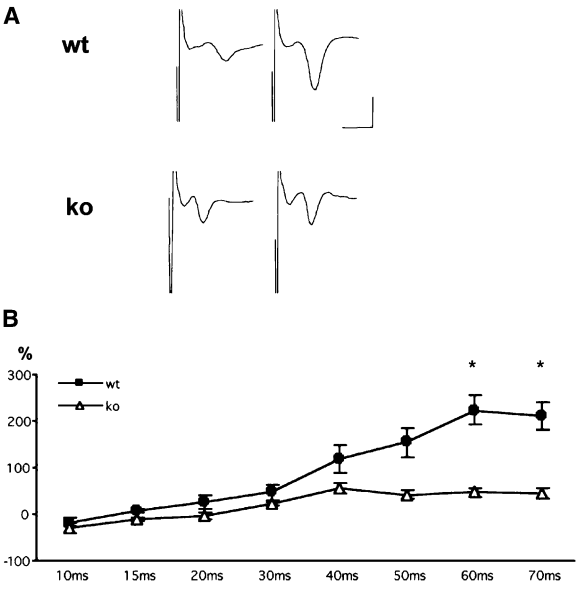


Figure 4. Field Potential Recordings Were Taken in CA1 Stratum Radiatum in Response to Paired Stimulation of CA3 Schaeffer Collaterals

(A) Representative recordings of paired-pulse stimulation of wt (top trace) versus *lynx1*$^{-/-}$ (ko) mouse slices (bottom trace). Synaptic responses from wt slices demonstrate a marked enhancement of the second pulse compared to the first (top). In contrast, synaptic responses from *lynx1*$^{-/-}$ slices showed a significant reduction of the second pulse relative to the first (bottom). Scale bars: vertical, 5 mV; horizontal, 5 ms.

(B) Quantitation of *lynx1*$^{-/-}$ slices (white) as compared to wt (black) mice exhibit reduced PPF ratios at intervals ranging from 30 to 70 ms as compared to wt mice. On the x axis, the interpulse interval (i.p.i.) from 10 to 70 ms at 10 ms increments is plotted. There was no significant difference at intervals less than 50 ms, n = 10 slices (ko), n = 5 slices (wt). For i.p.i. of 50 ms, p = 0.037; i.p.i. of 60 ms, p = 0.023; i.p.i. of 70 ms, p = 0.038.

Error bars show mean ± SEM.

*lynx1*$^{-/-}$ mice were analyzed in an elevated plus maze paradigm, a more sensitive test for anxiety. Mice were placed for 5 min in a plus-shaped maze that consisted of two open, white arms and two closed, black arms and were scored for entries into the open arm, entries into the closed arm, and time spent in the open arms. *lynx1*$^{-/-}$ mice displayed no significant differences from wild-type mice in any of these parameters (Figure 5D), although *lynx1*$^{-/-}$ mice displayed a nonsignificant increase in time spent in the open arm. We conclude from these studies that *lynx1*$^{-/-}$ mice manifest no differences in basal levels of anxiety. Thus, increased anxiety is unlikely to account for the freezing to tone observed in the fear-conditioning test.

### Enhanced Behavioral Nicotine Sensitivity in *lynx1* Null Mutant Mice

Nicotine receptor activation has been shown to stimulate locomotor activity in both rats and mice (Clarke and Kumar, 1983, King et al., 2004). To test whether behavioral responses to nicotine were altered in *lynx1*$^{-/-}$ animals, a series of locomotor tests were performed. To measure general activity levels in *lynx1*$^{-/-}$ mice, they were tested for diurnal locomotor activity over a 72 hr period (Figure 6A), as well as in a novel environment for 20 min (Figure 6B). No differences between *lynx1*$^{-/-}$ animals and wild-type littermates were observed in either diurnal locomotion (Figure 6A) or in response to novelty (Figure 6B), indicating that general activity levels were not significantly altered in *lynx1*$^{-/-}$ mice.

To test for sensitivity to nicotine, nicotine was administered to *lynx1*$^{-/-}$ animals and their wild-type littermates chronically (at least 6 weeks). Motor coordination and motor learning were assessed using an accelerating rotarod paradigm. *lynx1*$^{-/-}$ mice given saccharin alone in their drinking water showed no significant differences in rotarod performance from wild-type mice, either on the initial test day or on subsequent training days (Figure 6C). Although wild-type mice treated with nicotine plus saccharin (200 μg/ml nicotine in 2% saccharin) showed a trend toward improved performance on the accelerating rotarod compared to saccharin-treated wild-type mice in earlier trials, this difference was not significant (data not shown). In contrast, nicotine-treated *lynx1*$^{-/-}$ mice displayed a significant improvement in rotarod performance on the second day of training relative to similarly treated wild-type mice, demonstrating a greater effect of nicotine on motor learning in *lynx1*$^{-/-}$ mice than their wild-type littermates (Figure 6D). The heightened responsiveness of *lynx1*$^{-/-}$ mice to nicotine in this motor test is consistent with the observation that cultured neurons from *lynx1*$^{-/-}$ animals are also more responsive to nicotine (Figure 3) and is also consistent with our hypothesis that elimination of lynx1 alters nAChRs toward heightened receptor sensitivity.

### Neurons of *lynx1* Null Mutant Mice Are More Sensitive to Excitotoxic Insult

Treatment of cultured neurons with glutamate or glutamate receptor agonists results in an influx of $Ca^{2+}$ into the cell that can lead to cell death (McLeod et al., 1998). Pretreatment of neurons with nicotine prior to glutamate exposure can protect cells from glutamate-mediated excitotoxic cell death (Stevens et al., 2003). Since *lynx1*$^{-/-}$ cortical neurons showed increased $Ca^{2+}$ accumulation upon nicotine administration, we addressed whether *lynx1*$^{-/-}$ neurons are more vulnerable to glutamate toxicity and whether nicotine remains neuroprotective in the absence of lynx1. As shown previously, wild-type cultures exhibited a significant decrease in cell viability upon 100 μM glutamate treatment, and 1 hr pretreatment of nicotine protects wild-type neurons from cell death (Figures 7A and 7B, left panel) (Dajas-Bailador et al., 2000). In contrast, *lynx1*$^{-/-}$ neurons were more sensitive to glutamate-mediated excitotoxicity, and the neuroprotective effect of nicotine was completely abolished (Figures 7A and 7B, right panel). Previous studies have shown that nicotine-mediated neuroprotection usually occurs at low doses of nicotine, and the protective effect of nicotine is eliminated and can even result in more cell death with higher doses of nicotine. Consistent with the idea that the *lynx1*$^{-/-}$ cultures exhibit a shift in the dose-response curve to nicotine, these data suggest that the removal of lynx1 results in heightened sensitivity to nicotine and that a dose of nicotine that is normally neuroprotective is excitotoxic. These data also suggest that there may be an increased vulnerability to neurotoxic insult in *lynx1*$^{-/-}$ mice, mediated through elevations in $Ca^{2+}$ due to nAChR hyperactivation.

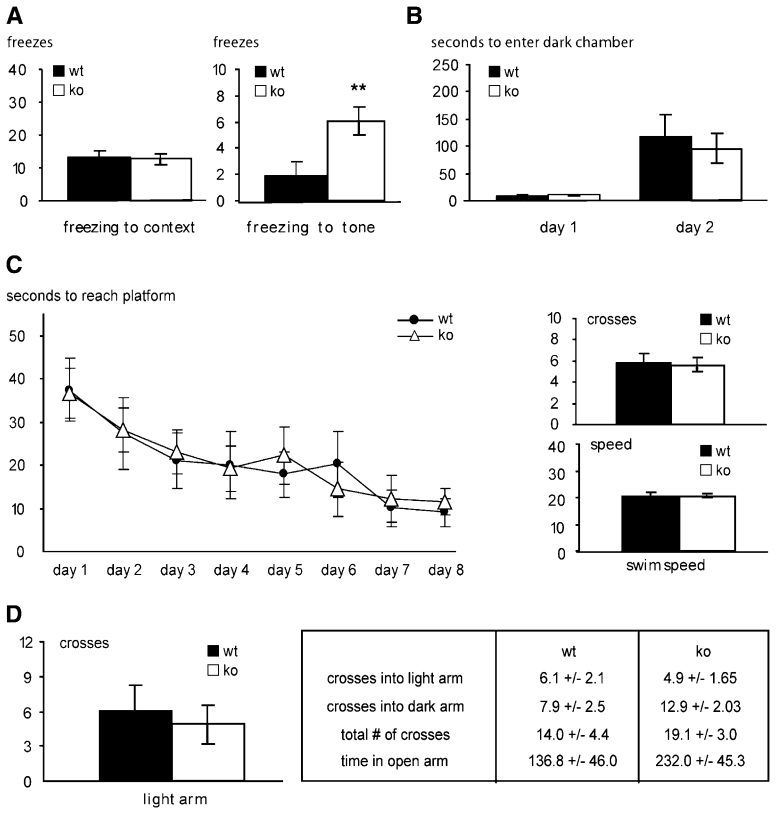


| | wt | ko |
|---|---|---|
| crosses into light arm | 6.1 +/- 2.1 | 4.9 +/- 1.65 |
| crosses into dark arm | 7.9 +/- 2.5 | 12.9 +/- 2.03 |
| total # of crosses | 14.0 +/- 4.4 | 19.1 +/- 3.0 |
| time in open arm | 136.8 +/- 46.0 | 232.0 +/- 45.3 |

Figure 5. Enhancement of Associative Learning Ability in *lynx1* Null Mutant Mice Observed in Fear-Conditioning Assays

(A) No differences in freezing were observed before conditioning between wt mice (black) and *lynx1*$^{-/-}$ (ko) mice (white) (data not shown). No differences were observed in freezing in the training cage 24 hr later (context), indicating there are no changes in contextual learning in *lynx1*$^{-/-}$ versus wt mice. *lynx1*$^{-/-}$ mice demonstrate a significant increase in freezing to tone as compared to wt mice (right). This was measured as the difference in freezing before and after tone presentation. $p = 5.5 \times 10^{-3}$, n = 8 (wt), n = 12 (ko).

(B) Passive avoidance learning analyses indicate no difference in performance in *lynx1*$^{-/-}$ mice versus wt mice.

(C) Morris water maze: no differences between *lynx1*$^{-/-}$ mice versus wt mice in learning to reach the hidden platform were observed. Learning curves as plotted from day 1 to day 8 were the same between *lynx1*$^{-/-}$ and wt mice (left). Furthermore, there were no differences when the platform was moved to another location (the transfer test) or in swim speed.

(D) Elevated plus maze test of anxiety. Mice were placed in an elevated plus maze, with two dark, closed arms and two light, open arms. Mice were placed in the maze for 5 min and scored for time spent in the light arms and entries into the light and dark arms. No significant differences were observed between genotypes for these parameters.

Error bars show mean ± SEM.

## Late-Onset Vacuolating Neurodegeneration in *lynx1* Null Mutant Mice

Given the enhanced vulnerability of cultured *lynx1* null mutant neurons to excitotoxic stimuli, we were next interested in determining whether the chronic disturbance of nAChR activity evident in *lynx1*$^{-/-}$ animals might result in cell loss in vivo. Thus, we performed an anatomic study using histological stains on

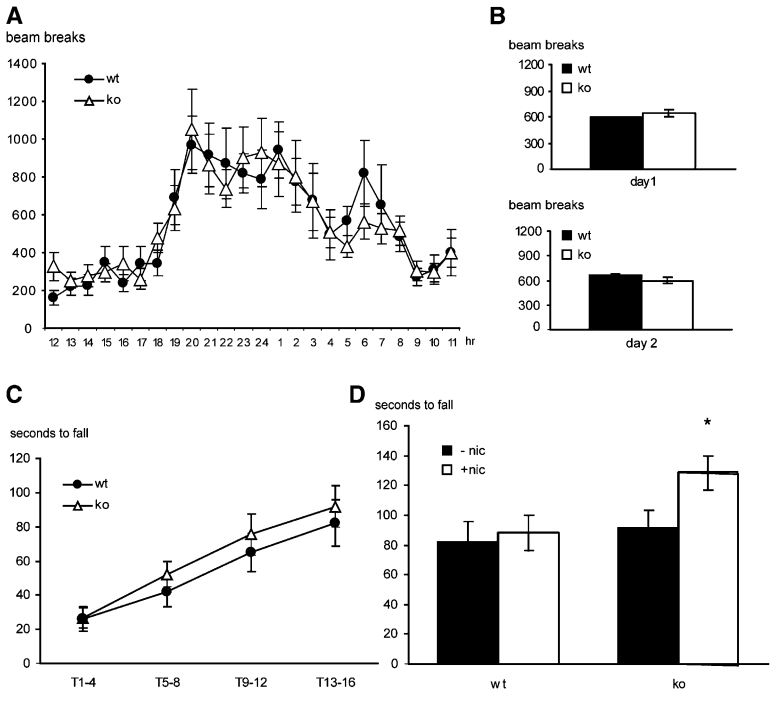


Figure 6. Enhancements in Nicotine-Mediated Motor Learning Performance in *lynx1* Null Mutant Mice

(A) Diurnal activity measured in a home cage environment over a 72 hr period. The number of beam breaks was measure and averaged across 3 days. No significant differences were observed between wt and *lynx1*$^{-/-}$ mice.

(B) Locomotor activity in a novel environment: Animals were placed in an open field box for a 20 min period of time, and the number of beam breaks was measured (upper). No significant differences were observed between *lynx1*$^{-/-}$ and wt mice on the initial day of testing (upper) or the second day (lower).

(C) *lynx1*$^{-/-}$ mice demonstrate no differences from wt in an accelerating rotoarod paradigm, indicating no differences in motor coordination or motor learning.

(D) *lynx1*$^{-/-}$ (ko) mice treated with nicotine showed significant differences in rotarod performance from untreated *lynx1*$^{-/-}$ or wt mice on the second day of training. No differences were observed on the initial day of testing (data not shown). Data plotted represents averages of trials 5–8 on day 2. p value = $5 \times 10^{-4}$.

Error bars show mean ± SEM.

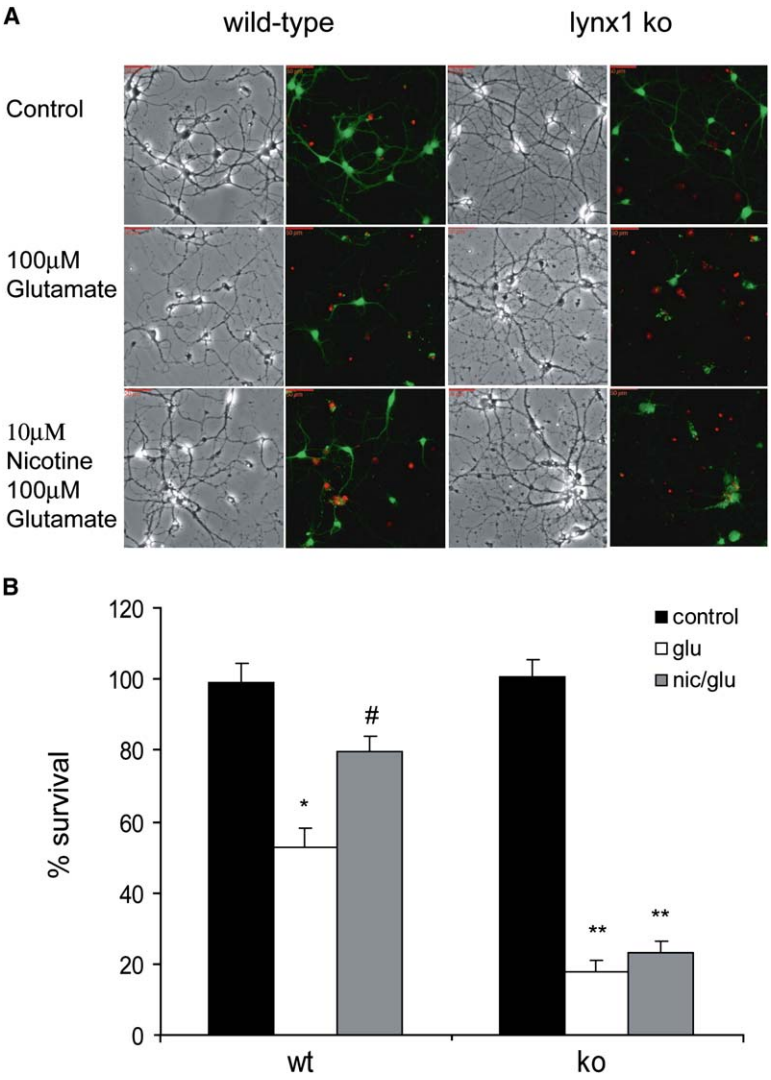


Figure 7. *lynx1* Null Mutant Cortical Cultures Exhibit Increased Excitotoxic Cell Death and a Loss of Nicotine-Mediated Neuroprotection

Nicotine-mediated neuroprotection against glutamate toxicity is abolished in primary cortical cultures from *lynx1*$^{-/-}$ mice. Cultures were pretreated with nicotine or buffer and then challenged with 100 μM glutamate. (A) Phase pictures and merged fluorescence images of calcein-AM and ethidium-stained wt cells demonstrate a reduction in live cells (green) and an increase in dead cells (red) in glutamate-treated cultures. Glutamate treatment reduced cell survival (56%), and nicotine protected neurons from glutamate-mediated cell death (77%). Phase pictures and merged images from *lynx1*$^{-/-}$ (ko) cultures demonstrate that there is an increase in glutamate-induced cell death (18%) compared to wt. In addition, nicotine is not protective in the absence of lynx1 (23%). (B) Quantitation of cell death in wt and *lynx1*$^{-/-}$ (ko) cultures. Live cells are stained green throughout the cell body and projection. Dead cells exhibited red staining or weak punctuated green staining. A one-way ANOVA was used to determine significance. *Glutamate versus control ($p < 0.005$; LSD post hoc test). #Nicotine pretreatment versus glutamate alone ($p < 0.005$; LSD post hoc test). **In *lynx1*$^{-/-}$ cultures, both glutamate treatment and nicotine pretreatment versus glutamate treatment in wt cultures. n = at least 200 cells/condition, mean ± SEM. Error bars show mean ± SEM.

*lynx1*$^{-/-}$ versus wild-type coronal brain sections. We detected no significant difference between *lynx1*$^{-/-}$ and wild-type mouse brains at 9 months of age (data not shown). However, inspection of brains from *lynx1*$^{-/-}$ animals taken at 12 months revealed the presence of large vacuoles in the dorsal striatum (Figure 8A) and isolated brainstem regions (data not shown). Most of these lesions were present in the pinker, eosinic areas of the sections, indicating that the degeneration was occurring within axonal tracts within the striatum (Figure 8B). Further evidence of axonal degeneration was found in the cerebellum (Figure 9A), where nAChRs have been demonstrated (Kaneko et al., 1998) and where vacuolation was found to occur at high levels within the neuropil of the cerebellar lobes (Figures 9A and 9B) and the superior cerebellar peduncle (Figure 9C).

To determine whether the vacuolating phenotype of *lynx1*$^{-/-}$ brains might be affecting neurons, we performed DeOlmos amino cupric silver staining for disintegrative neuronal degeneration on cross-sections of 12-month-old mutant and wild-type brains. Consistent with the vacuolation within axon-dense regions, we observed a predominance of silver staining within axon tracts coursing through the striatum as well as silver labeling within the corpus callosum (Figure 8C) and in the cerebellum (Figure 9D), demonstrating increased neuronal degeneration within aging *lynx1* mutant mouse brains.

To assess the progressive nature of this degenerative phenotype, we measured the number of lesions present in the striatum of *lynx1* mutant mouse brains from 6 to 18 months of age (Figure 10). We quantitated the number of vacuoles within the striatum of each mouse brain and observed an age-dependent increase in vacuolation, first detectable in 12-month-old *lynx1*$^{-/-}$ mice and increasing at 15 and 18 months of age (Figure 10A). We also performed quantitative analyses of the silver-stained sections, revealing a significant increase in labeling of *lynx1*$^{-/-}$ as compared to wild-type brains in the dorsal striatum (Figure 10B, left) and the medial corpus callosum (Figure 10B, right). Our results are consistent with previous reports that hyperactivation of nAChRs can result in CNS damage and support the hypothesis that persistent elevations in nicotinic cholinergic signaling make a contribution to neuronal degeneration within aging *lynx1*$^{-/-}$ mouse brains.

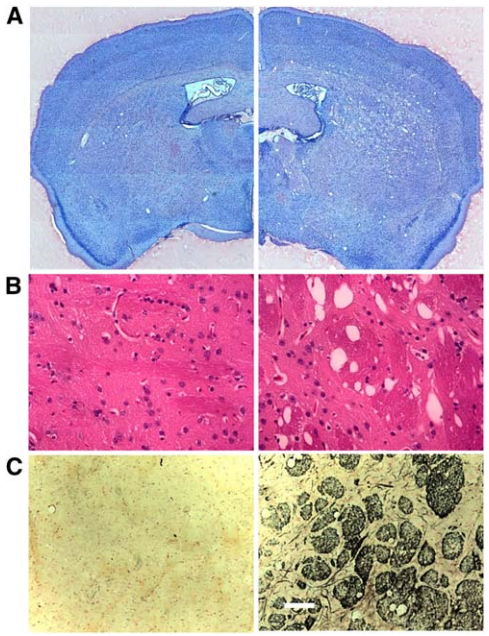


Figure 8. *lynx1* Null Mutant Mice Undergo Degeneration within the Dorsal Striatum

(A) Light micrographs of H&E-stained coronal sections of wt (left) and *lynx1*$^{-/-}$ (right) mouse brains indicate a vacuolating phenotype in 1-year-old *lynx1*$^{-/-}$ brains. Wild-type and *lynx1*$^{-/-}$ brains were analyzed at the same level in a cross-section of the striatum. Vacuolation was observed predominantly in the dorsal striatum ([A], right). Montage of ~40 micrographs taken at 20× magnification.

(B) Individual micrograph of the striatum of H&E-stained coronal sections, as in (A), reveals vacuolation, especially in the darker, eosinic regions that label axonal tracts coursing through the striatum in *lynx*$^{-/-}$ (right) but not wt (left) brains. 20× magnification.

(C) DeOlmos silver cupric staining of degenerating neurons indicates increased staining in *lynx1*$^{-/-}$ (right) as compared to wt brain sections (left). Silver grain deposition is preferentially localized to axon bundles coursing though the striatum, reaching to and from the cerebral cortex. 20× magnification.

## Neurodegeneration in *lynx1* Null Mutant Mice Is Exacerbated by Nicotine

If increased activity of nAChRs in *lynx1* mutant mice is responsible for this vacuolating phenotype, then pharmacologic manipulations that influence the activity of these receptors might alter the course of degeneration. To test this idea, a solution of nicotine and saccharin, or saccharin alone, was administered to cohorts of *lynx1*$^{-/-}$ animals and their wild-type littermates through their drinking water. Administration of the nicotine solution was begun at 8 months of age, before the observed onset of degeneration, and continued for a period of 10 months. As shown in Figure 10C, there were no significant differences in vacuolation in the striatum of saccharin- versus nicotine/saccharin-treated wild-type mice (left). However, in *lynx1*$^{-/-}$ mice treated with the nicotine solution, we observed a significant increase in vacuolation (Figure 10C, right). These data strongly suggest that the degenerative phenotype we observed in *lynx1*$^{-/-}$ brains results from increased nAChR activity, consistent with the enhanced vulnerability of *lynx1*$^{-/-}$ neurons to excitotoxic stimuli and the loss of neuroprotective effect documented above (Figure 7).

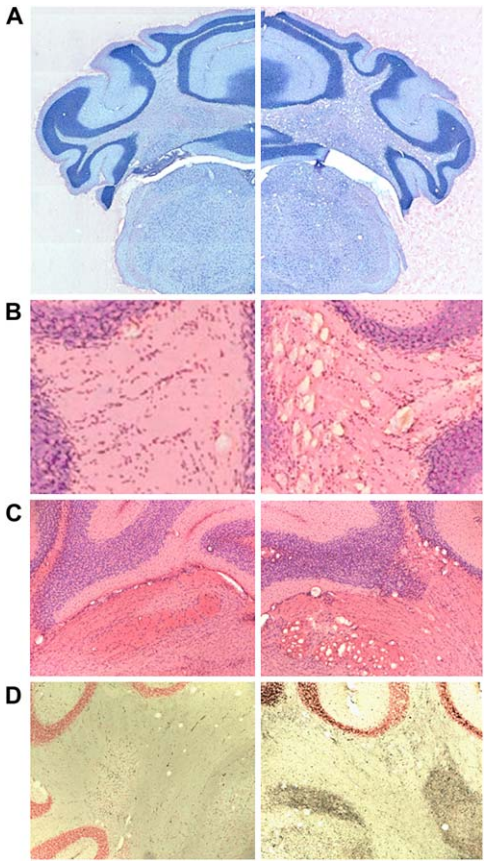


Figure 9. Cerebellar Degeneration Preferentially Affects Axonal Tracts in *lynx1* Null Mice

(A) Coronal brain sections of *lynx1*$^{-/-}$ (right) and wt (left) 1-year-old mice through the cerebellum stained with H&E stain indicate a vacuolating degeneration in the neuropil in *lynx1*$^{-/-}$ but not wt mouse brains. Bregma, −6.56; interaural, −2.76. Montage of H&E-stained brain sections were imaged at 10× magnification and stitched together with Zeiss KS400 software.

(B) High-power magnification of (A) in the neuropil of the interior cerebellum in wt (left) and *lynx1*$^{-/-}$ (right) mice at 20× magnification.

(C) Images of the superior cerebellar peduncle in wt (left) and *lynx1*$^{-/-}$ (right) mouse brains. Sections at bregma −5.88, interaural −2.08 mm indicate a vacuolating degeneration in the pink, eosinic region at the border between the cerebellum and the brainstem, indicating a preferential loss of axons in *lynx1*$^{-/-}$ and not wt mice. Micrographs imaged at 20× magnification.

(D) Silver staining of degenerating neurons indicates high levels of silver stain in the cerebellum in *lynx1*$^{-/-}$ (right) but not wt (left) mouse brains. 20× magnification.

## Neurodegeneration in *lynx1* Null Mutant Mice Requires nAChRs

Our previous in vitro studies, including single-channel recordings of nAChR activity with and without lynx1, demonstrated a direct effect of lynx1 on nAChRs. If the degenerative phenotype of *lynx1*$^{-/-}$ mice reflects the loss of its ability to modulate nAChR activity, then deletion of nAChRs would be expected to rescue the degenerative phenotype observed in *lynx1*$^{-/-}$ animals. To test this idea, we crossed the *lynx1* null mutation onto nAChR mutant backgrounds to prepare double-mutant animals in which the effect of nAChRs on the *lynx1*$^{-/-}$ degenerative phenotype could be assessed. As shown in Figure 10D, a significant reduction in the number of

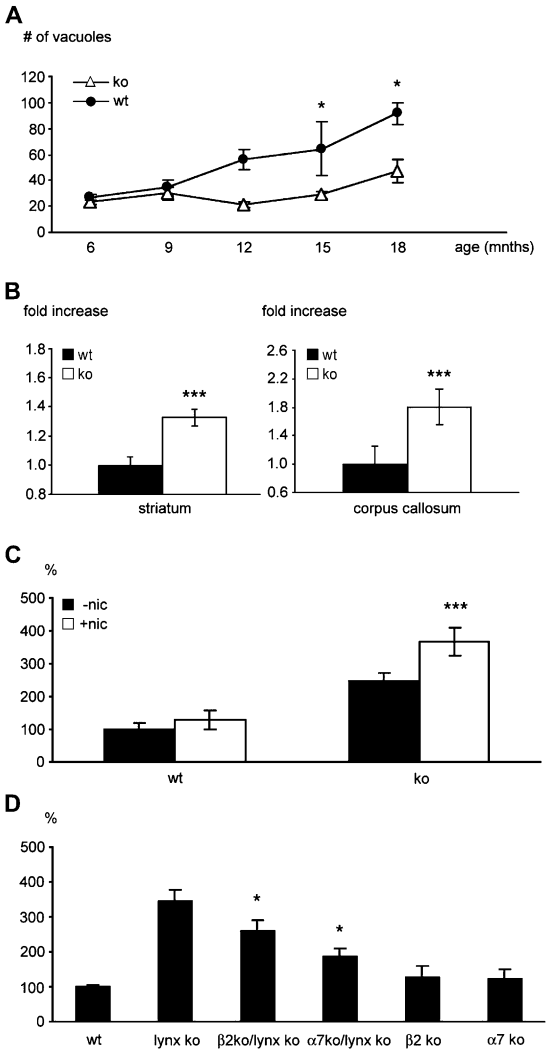


Figure 10. nAChRs Are Involved in the Vacuolation Observed in *lynx1* Null Mutant Mice

(A) Vacuolation is observed in the striatum of *lynx1*$^{-/-}$ (ko) mice (white triangles) at the age of 12 months onward as compared to wt mice (black squares). At 6 months, n = 3 (wt), n = 3 (ko); at 9 months, n = 6 (wt), n = 6 (ko); at 12 months, n = 5 (wt), n = 10 (ko), Student's t test, p = 2.8 × 10$^{-6}$; at 15 months, n = 3 (wt), n = 3 (ko), p = 0.037; at 18 months and older, n = 5 (wt), n = 5 (ko), p = 6 × 10$^{-5}$, ko values compared to wt values.

(B) Quantitative analysis of DeOlmos silver cupric staining of *lynx1*$^{-/-}$ versus wt brains. Light micrographs were taken under the same conditions for each brain in the dorsal midbrain. Quantitation of silver grains indicated a significantly higher level of staining in *lynx1*$^{-/-}$ sections (white) versus wt sections (black) in the dorsal striatum (left) or in the corpus callosum (right). Striatum, p = 0.003; corpus callosum, p = 7.2 × 10$^{-6}$.

(C) Chronic nicotine treatment exacerbates vacuolation in *lynx1*$^{-/-}$ (ko) but not wt striata. Nicotine-treated mice (200 μg/ml in 2% saccharin, white) or a control solution (2% saccharin, black). Nicotine-treated *lynx1*$^{-/-}$ mice show a significant increase in vacuolation as compared to untreated or treated wt mice. n = 3 (ko-nic), 3 (ko+nic), 3 (wt-nic), 2 (wt+nic). Student's t test, wt-nic versus ko+nic, p = 8.6 × 10$^{-3}$; ko+nic versus ko-nic, p = 0.009; wt-nic versus ko-nic, p = 0011.

(D) nAChRs null mutant mice provide a partial rescue of the vacuolating phenotype observed in striata of *lynx1*$^{-/-}$ mice. Brains of *lynx1*$^{-/-}$/α7 *nAChR*$^{-/-}$ mice show an almost complete rescue of vacuolation as compared to those of *lynx1*$^{-/-}$ mice. p < 0.05 (ANOVA LSD post hoc analysis). The striatum of *lynx*$^{-/-}$/β2 *nAChR*$^{-/-}$ double mutant mice showed a reduction in vacuolation as compared to that of *lynx1*$^{-/-}$ mice (p = 0.003), though to a much smaller degree than the rescue achieved with the *lynx1*$^{-/-}$/α7 *nAChR*$^{-/-}$ mice (p = 4.2 × 10$^{-4}$). n = 5 (wt), 9 (*lynx1*$^{-/-}$), 11 (*lynx1*$^{-/-}$/β2 *nAChR*$^{-/-}$), 5 (*lynx1*$^{-/-}$/α7 *nAChR*$^{-/-}$), 2 (β2 *nAChR*$^{-/-}$), 2 (α7 *nAChR*$^{-/-}$). wt versus *lynx1*$^{-/-}$ (p < 0.001).

Error bars show mean ± SEM.

lesions present in the striatum at 15 months of age was observed in both *lynx1*$^{-/-}$/β2 *nAChR*$^{-/-}$ and *lynx1*$^{-/-}$/α7 *nAChR*$^{-/-}$ double mutant mice relative to their littermates bearing only the *lynx1*$^{-/-}$ mutation. It is notable that the rescue of degeneration in *lynx1*$^{-/-}$/α7 *nAChR*$^{-/-}$ was greater than that observed *lynx1*$^{-/-}$/β2 *nAChR*$^{-/-}$ double mutant animals, since α7 nAChRs have a greater $Ca^{2+}$ conductance than β2 nAChRs (Berg and Conroy, 2002). These data demonstrate that lynx1 action in vivo requires α7 and β2 nAChRs. Taken together with the in vitro data presented previously and in the current study and the differential effects of nicotine treatment on motor learning and neurodegeneration we have observed in *lynx1*$^{-/-}$ animals (Figures 6 and 10), the rescue of the degenerative phenotype in lynx1 mutant animals by deletion of *nAChRs* provides a strong argument for a direct role of lynx1 in modulation of nAChR activity in vivo.

## Discussion

The analyses of *lynx1* null mutant mice we present in this study reveal several important new features of lynx1 function and its impact on cholinergic activity in the central nervous system. Whole-cell recordings of responses to nicotine pulses in brain slices show that loss of lynx1 results in hypersensitivity of nAChRs to nicotine and to prolonged nAChR receptor activation. These changes are sufficient to raise intracellular $Ca^{2+}$ levels in *lynx1* null mutant but not in wild-type neurons in response to acute or maintained nicotine. *lynx1* null mutant mice exhibit a reduction in paired-pulse facilitation ratios in brain slices, indicating increased synaptic efficacy within neuronal ensembles. *lynx1* mutant mice perform better than wild-type littermates on specific tasks of associative learning, and *lynx1* mutant mice are more responsive to nicotine in a motor-learning paradigm. Finally, loss of lynx1 modulation leads to increased vulnerability to excitotoxic stimuli and loss of the neuroprotective effect of nicotine. Accordingly, aging *lynx1* null mutant mice suffer from a progressive, vacuolating degeneration of the brain that is exacerbated by nicotine administration and rescued by null mutations in nAChRs.

The involvement of lynx1 in nAChR modulation demonstrated here has important consequences for studies of nAChR function in the brain. The properties of lynx1 action in vitro are supported by the patch-clamp studies reported here, which demonstrate an ~10-fold shift in the dose-response relationship of nAChRs to nicotine toward more sensitive receptors in *lynx1* mutant mouse brain slices as compared to those of wild-type mice. Changes in nicotine sensitivity confer on the organism marked physiological effects that correlate with the degree of change in the $EC_{50}$. Mutations in nAChRs inducing a greater than 100-fold shift in $EC_{50}$ in ooctyes cause neuronal cell loss and neonatal death (Labarca et al., 2001). More moderate nAChR mutations that confer

a shift in the $EC_{50}$ of 7- to 30-fold in ooctyes result in seizure susceptibility (Fonck et al., 2005; Bertrand et al., 1998) and increased addictive propensity, but no apparent neonatal loss of neurons. Our results reveal that lynx1 removal causes a comparatively subtle gain-of-function of wild-type nAChRs in vivo, perhaps allowing elucidation of cholinergic processes that might otherwise be difficult to discern in vivo. For example, the ability of lynx1 to modulate nAChR kinetics, agonist affinity, and desensitization may help to explain the discrepancy between dose-response curves and $EC_{50}$ values of nAChRs in vivo, where lynx1 is generally present, as compared to results obtained using heterologous expression systems that do not include lynx1 (Quick and Lester, 2002; Truong et al., 2001).

Although our studies cannot decisively identify the biophysical mechanism of lynx1 action, several aspects of our data are consistent with earlier conclusions that lynx1 affects nAChR desensitization. First, nicotine responses in *lynx1* null mutant brain slices decay back to baseline more slowly than those in wild-type mice (Figure 2). Second, ~1 hr exposure to 1 mM nicotine produces a sustained $Ca^{2+}$ increase in *lynx1* null mutant but not wild-type neurons (Figure 3); thus, a regimen of nicotine administration that desensitizes nAChRs in wild-type mice (Vijayaraghavan et al.,1992) allows persistent activation of nAChRs in *lynx1* mutant cells. Desensitization is an overall term for a complex and incompletely described series of conformational transitions that favor bound agonist but have closed channels. Compared with the transition to the open state, transitions to desensitized states have a higher activation energy but result in more stable states. As a result, nicotinic receptors enter these desensitized states in response to maintained exposure to ACh, nicotine, or other agonists (Lester et al., 2004, Buisson and Bertrand, 2001). Long-term nicotine exposure has been shown to shift the $EC_{50}$ to more sensitive receptors and slow the onset of desensitization, through a mechanism involving isomerization of nAChRs from a low to high affinity state. Nicotinic receptor desensitization does not directly involve changes in receptor number (Marks et al., 1992) or expression of receptors at the cell surface (Whiteaker et al., 1998). Desensitized states are primarily reached from the open state, so that hypersensitivity to agonists is often accompanied by hypersensitivity to desensitization (for instance, see Fonck et al., 2005). Desensitization may have the selective advantage of protecting neurons against excitoxicity due to prolonged agonist exposure. We propose that, in addition to its direct effects on sensitivity (Figures 2A, 2C, 3C, and 3D), lynx1 also acts to change the relative stability and/or transition energies among activated and desensitized states. Thus, we propose that lynx1 acts as an allosteric modulator of nAChR(s) to maintain low ACh sensitivity and a good safety margin against agonist overstimulation of these critical receptors.

Such shifts in agonist sensitivity and desensitization kinetics reveal downstream consequences for removal of nAChR modulators in $Ca^{2+}$ imaging studies conducted on primary neuronal cultures from *lynx1* null mutant mice. Under our conditions, only cultures from *lynx1* mutant mice display a dose-dependent increase in intracellular $Ca^{2+}$ upon nicotine treatment. No nicotine-mediated increases in $Ca^{2+}$ were observed in wild-type cultures, supportive of hypersensitivity to nicotine of nAChRs in *lynx1* mutant cultures. Hypersensitivity to $Ca^{2+}$ increases were observed following nicotine pulses in mice with a hyperactivating mutation of the $\alpha$4 nAChR subunit as well (Tapper et al., 2004), supporting the idea that nAChR activation can induce rises in $Ca^{2+}$ levels, whether via nAChR receptor channels themselves or through alternate means such as voltage-dependent $Ca^{2+}$ channel activity (Rathouz and Berg, 1994) or $Ca^{2+}$-induced $Ca^{2+}$ release from intracellular stores (Sharma and Vijayaraghavan, 2003).

Elevations in $Ca^{2+}$ levels, such as those observed in *lynx1* null mutant neurons, can have significant consequences for synaptic signaling (Dittman et al., 2000). The reduction of PPF ratios in *lynx1* mutant mice is an indicator of enhanced synaptic efficacy within neuronal ensembles, which is thought to result from a depletion of readily available vesicle pools in response to a large initial influx of $Ca^{2+}$. This can inhibit facilitation of the second stimulus, even under conditions of higher $Ca^{2+}$ concentrations. nAChRs localized on presynaptic terminals are able to regulate $Ca^{2+}$ entry, and thus NT release, via $Ca^{2+}$ influx directly or by membrane depolarization. In vivo, nicotinic currents desensitize rapidly (Wooltorton et al., 2003; Marks et al., 1994). Thus, we infer that, without the desensitizing influence of lynx1, nAChRs can make greater contributions to elevations of $Ca^{2+}$ levels, resulting in increased vesicular fusion and more efficient synaptic signaling. This is supported by evidence that conditions that favor nAChR desensitization prevent facilitation of paired nicotine responses by the regulation of intracellular $Ca^{2+}$levels (Klein and Yakel, 2005) and with published reports of nicotine enhancing the presynaptic release of NTs (Mansvelder et al., 2002; McGehee et al., 1995) and synaptic efficacy in the developing hippocampus (Maggi et al., 2004).

The increased tone-paired freezing observed in these animals is consistent with the reduction of PPF, since fear conditioning is correlated negatively with PPF in wild-type mice (Shinnick-Gallagher et al., 2003). Enhancements in cue-associated freezing observed in *lynx1* mutant mice are indicative of improvement in complex forms of learning and memory (Schafe et al., 2001). We believe this to be due to an increase in learning, rather than due to elevations in anxiety in the mutant mice, as there were no significant differences in elevated plus maze performance. Sensory and motor alterations could produce freezing behavior that mimics improved fear-conditioned memory. However, as the animals freeze to the identical context and to the tone, but not in the contextually altered environment on the test day, we conclude that the alterations in sensory or motor abilities cannot account for the increased freezing to tone in *lynx1* mutant mice (Crawley, 2000). Additionally, the fact that *lynx1* mutant animals are able to learn on the rotarod task further supports this, as the rotarod task is dependent on visual rather than auditory cues. Our data support a model in which *lynx1* mutant mice have a heightened sensitivity to nicotine, leading to enhanced synaptic plasticity and increases in associative learning. The results obtained in the rotarod test that revealed that, in contrast to wild-type mice, motor learning in *lynx1* mutant mice is sensitive to chronic exposure to

nicotine support this and are consistent with the involvement of nAChR activation in behavior (Gould and Wehner, 1999).

Both in vivo and in vitro studies have shown that α7 and α4/β2* nAChRs contribute to the neuroprotective effects of nicotine in neurons. We have shown here that primary neuronal cultures made from *lynx1* mutant mice show a greater susceptibility to the excitotoxic effects of glutamate and loss of the neuroprotective effect of nicotine observed in wild-type neurons. While the elevation of $Ca^{2+}$ levels observed in *lynx1* mutant neurons can have positive effects, such as improved learning and greater capacity for synaptic alterations, elevated $Ca^{2+}$ levels are strongly correlated with susceptibility to excitotoxic cell death. The loss of nicotine-mediated neuroprotection in *lynx1* mutant cultures is consistent with previous in vitro studies that show that nicotine-mediated neuroprotection is generally observed at low doses of nicotine, whereas high concentrations of nicotine can exacerbate cell death. The neurotoxic effect of chronic hyperstimulation has been demonstrated for both the α4 and α7 nAChR subunits, where hyperactivating mutations lead to neurodegeneration. Given these precedents, we propose that the degenerative phenotype observed in mice lacking lynx1 is due to the loss of lynx1 modulation of nAChRs. Chronic nAChR-dependent elevations in intracellular $Ca^{2+}$ levels contribute to the probability that $Ca^{2+}$ influx as a result of normal activity will exceed the $Ca^{2+}$-buffering capacities of the cell, leading to neuronal vulnerability. Thus, the probability that a neuron will exceed the threshold for excitotoxic death (Clarke and Lumsden, 2005) is increased in *lynx1* mutant animals, resulting in a progressive degenerative phenotype that is significant, although not as severe as that seen with hypersensitive mutations of nAChRs.

The greater ability of *α7 nAChR* as compared to *β2 nAChR* null mutant mice to rescue neurodegeneration in *lynx1* mutant mice is consistent with this idea, since α7 nAChRs are more permeable to $Ca^{2+}$ than β2 nAChRs (Fucile, 2004; Berg and Conroy, 2002). However, since intracellular $Ca^{2+}$ may rise through alternative means, the vacuolation in *lynx1* null mutant mice may not depend solely of the relative extent of $Ca^{2+}$ flux through specific nAChR subunits. For example, it has been postulated that α7* nAChRs are responsible for $Ca^{2+}$ influx through its channels, whereas β2* subunit-containing nAChRs depolarize the membrane and thereby activate voltage-gated $Ca^{2+}$ channels that allow $Ca^{2+}$ entry (Tsuneki et al., 2000). We propose that the desensitizing influence of lynx1 on nAChRs provides a high safety margin for exposure to ACh or nicotine by causing a shift toward less sensitivity to ACh and more rapid desensitization, thus reducing the available pool of receptors that can be activated by successive stimuli. Our data suggest that one of the major roles of lynx1 within the CNS is to buffer the cell from destructive excitotoxic events that must occur during the normal lifetime of the animal.

This study indicates that lynx1 acts as a modulatory component on nAChR receptors to maintain receptor activity within a narrowly defined window that is beneficial for neuronal function. A molecule acting in such a capacity can have important neurological consequences. For instance, in the human epilepsy disorder ADNFLE, alterations in desensitization kinetics and gating characteristics of nAChRs can shift the balance between excitation and inhibition too far toward excitation. The *C. elegans* mutant *odr2*, a related family member to *lynx1*, causes olfactory deficits (Chou et al., 2001), and mutations in the secreted lynx1 homolog SLURP-1 cause changes in agonist affinity of nAChRs, which result in an inflammatory disorder of the skin, Mal de Meleda (Chimienti et al., 2003). It seems highly probable that other members of the *lynx1* gene family, and indeed other prototoxin-like molecules, also function as modulatory components of other CNS receptors to maintain activity within this narrowly defined window. Given the vital function of lynx1 in modulating nicotinic tone and fine-tuning the activity of neuronal ensembles demonstrated in this study, we believe lynx1 will be an important component in many aspects of cholinergic function, both in the CNS and in the periphery where lynx1 expression has been demonstrated (Sekhon et al., 2005).

The effect of lynx1 on the kinetic properties of nAChRs has important therapeutic implications. lynx1 provides a novel target for drug discovery that could be of value for identifying compounds to treat cognitive loss in aging or as a consequence of dementia. This strategy presents advantages to current treatments for neurological disorders such as Alzheimer's disease or Parkinson's disease that seek to enhance cholinergic activity by inhibition of acetylcholinesterase (Trinh et al., 2003) or increases in agonist concentration (Kelton et al., 2000; Chorvat et al., 1998), since increases in agonist binding can lead to downregulation of nAChR function by desensitization. Targeting allosteric modulators of nAChR could circumvent such problems by increasing signaling of nAChRs without triggering desensitization or compensatory downregulation (Hurst et al., 2005; Pereira, et al., 2002; Maelicke et al., 2000). Drugs that act on lynx1 modulators could allow access to circuits within the brain that previously have been intractable through direct targeting of cholinergic receptors. Our data point to lynx1 as a promising new target for pharmacologic manipulation of nAChR function in vivo, while providing a cautionary note that the benefits of pharmacologic inhibition of lynx1 must be weighed against the degenerative effects of chronic nAChR activation.

## Experimental Procedures

### Targeting Mutagenesis and Detection

Gene-specific primers were used to amplify an frt-neo-recA plasmid using a bacterial recombination method described in Yu et al. (2000). Standard methods were used for gene targeting (see the Supplemental Data). Ssp1-digested genomic DNA probed with a 3′ external probe recognized a 12 kb band (wt) and a 9 kb recombinant band. Western analysis utilized purified anti-lynx pAb to probe extracts from *lynx1*$^{-/-}$, *lynx1*$^{+/-}$, and *lynx1*$^{+/+}$ forebrain.

### Patch-Clamp Electrophysiology in Medial Habenula

See Supplemental Data and Tapper et al. (2004). Internal pipette solution, in mM: 100 mM $K^+$ gluconate, 0.1 $CaCl^{2+}$, 1.1 EGTA, 5 $MgCl^{2+}$, 10 HEPES, 3 ATP, 3 phosphocreatine, 0.3 GTP, pH to 7.2 with KOH. Somatic whole-cell recordings were made from visually identified habenular neurons from P14–P17 mice. For nicotine application, a glass pipette connected to a relay-controlled pressure device was moved to within 20 μm of the recorded cell using a piezoelectric manipulator, and nicotine was applied for 250 ms and retracted. 10 μM mecamylamine was bath perfused.

### $Ca^{2+}$ Imaging

Mixed cortical cultures (11–13 days old) were made from E16–E18 fetal mice as has been described (Stevens et al., 2003); see the Supplemental Data. After nicotine or HBS pretreatment for 1 hr, cells were loaded with 2 μM fluo-3 for 10 min RT. Images were obtained using a 20× objective on a Nikon TE300 inverted microscope equipped with a cooled CCD camera (Hamamatsu orca), collected at 2 s intervals and adjusted for the level of background intensity, digitally colored and analyzed using IPLab software, measuring somatic pixel density, adjusted against background, for over 40 neurons per genotype/condition.

For acute nicotine experiments, $Ca^{2+}$ influx was determined as the change from basal fluorescence upon a 10 s application of 1 mM nicotine ([stimulated level − basal level]/basal level of fluorescence), quantitated as described by Vijayaraghavan et al. (1992). *lynx1*$^{-/-}$, n = 18; wt, n = 24. Dose-response measurement: extracellular $Ca^{2+}$ was increased to 3 mM and 0 mM $MgCl^{2+}$ to increase the changes observed in $Ca^{2+}$ influx at lower doses. Nicotine doses ranged from 1 mM to $1 \times 10^{-6}$ mM. The wt cultures showed no significant change with 1 mM nicotine ($\Delta F/F = 0.04$, n = 24 cells), so lower doses of nicotine were not tested. These experiments were conducted in three different cultures. 1 mM, n = 32 cells; 0.1 mM, n = 20 cells; 10 μM, n = 32 cells; 1 μM, n = 28 cells.

### Hippocampal Slice Electrophysiology

CA3 to CA1 field potentials were recorded in P28–P35 transverse hippocampal slices in response to monopolar stimulation of 50%–60% maximum response. Two stimuli were applied with a minimum interval delay ranging from 10 ms to a maximum delay of 70 ms. For details, see the Supplemental Data.

### Behavioral Tests

#### *Fear Conditioning*

Mice were presented with two pairings of the tone with foot shock (0.5 mA, 2 s). For contextual conditioning, freezing was scored for 5 min in the conditioning chamber. For the cued test, mice were placed into a different cage, and a novel odor (orange extract) was added to the context. Mice were scored for freezing in the altered context for 3 min before and 3 min during presentation of the tone (cued conditioning test). For details, see the Supplemental Data. Passive avoidance learning and Morris water maze learning, see the Supplemental Data. Rotarod: *lynx1*$^{-/-}$ and wt mice were administered either 2% saccharin or 200 mg/ml of nicotine hemisulfate salt in 2% saccharin through their drinking water. Adult mice were tested in squads of four, for eight trials per day on consecutive days. Animals were tested with an accelerating paradigm of a 1 RPM starting speed and a rate of acceleration of 0.1 RPM/s. Animals were scored for time to fall or time to stop running.

### Assessment of Neurotoxicity

Nicotine (10 μM) or buffer preincubation was carried out for 1 hr at 37°C, and 100 μM glutamate or buffer treatment was assessed after 18–20 hr. Cells were treated with 0.16 mM calcein-AM-0.36 mM ethidium homodimer in HBS 2.1 (40 min, RT). Live cells were stained green throughout the soma and projections, whereas dead cells had red staining only in the nucleus or highly punctate green staining. Neurotoxicity was calculated as percentage survival [live cells/(live + dead cells)] relative to control cells. Four to six coverslips were examined per treatment, and a total of 10 to 15 randomly selected fields (10×) were captured using IPLab software. At least 200 cells were counted per condition, and each experiment was repeated in at least two different cultures.

### Histology

Micrographs of H&E-stained coronal sections were taken with a Zeiss Axioplan2 microscope with a 10× objective, and the individual pictures were stitched together to create a montage. For details, see the Supplemental Data. For quantitation of the vacuolation, sections were picked at the same rostral-caudal level through the striatum. Bregman 0.00, interaural 3.80 mm. The number of gaps in the neuropil of at least a cell body in diameter were counted to yield the number of vacuoles per striatal hemisphere. For nicotine-treatment, drinking water contained 200 μg/ml nicotine in 2% saccharin, starting at 8 months for a 10 month period of time. *α7* and *β2 nAChR*$^{-/-}$ mice were obtained from the Beaudet laboratory and bred to C57Bl6/J6 *lynx1*$^{+/-}$ mice. Fifteen-month-old mouse brains were drop-fixed in 4% paraformaldehyde in PB. Wild-type, n = 5; *β2 nAChR*$^{-/-}$*/lynx1*$^{-/-}$, n = 6; *α7 nAChR*$^{-/-}$*/lynx1*$^{-/-}$, n = 5; *α7 nAChR*$^{-/-}$, n = 2; *β2 nAChR*$^{-/-}$, n = 2. Silver staining of degenerating neurons was conducted by a modification of DeOlmos amino cupric silver stain (Neurosciences Associates, Knoxville, TN). Density measures (NIH Image) of 20× dorsal striatal micrographs were normalized against the wt.

### Supplemental Data

The Supplemental Data for this article can be found online at http://www.neuron.org/cgi/content/full/51/5/587/DC1/.

### Acknowledgments

We wish to thank A.L. Beaudet for generously providing the α7 and β2 nAChR mutant mice used in these experiments. Special thanks to Dr. Andreas Walz, Dr. S. Selesnick, and Dr. P. Gutin. For helpful scientific discussions and/or technical support, thanks to C. Fletcher, R.A. Lester, A.B. Tekinay, R. Nashmi, A. Tapper, R. Pantoja, F. Moss, and B. Cohen and other members of HAL lab; B. Switzer of NSA, A. Kolar, S. Krueger, and A. Aslantas. Support for M.R.P., S.L.K., B.J.C., and T.R.S.: DA00436, DA15241, and AA15632; for J.M.M., NIH CA09673; for N.H., J.M.M., and I.I.-T., HHMI and NIH NIH R21 NS047751; for H.A.L. and C.X., DA-17279 and CA Tobacco-Related Disease Research Project.

Received: December 21, 2004
Revised: October 21, 2005
Accepted: July 19, 2006
Published: September 6, 2006

### References

Abrous, D.N., Adriani, W., Montaron, M.F., Aurousseau, C., Rougon, G., Le Moal, M., and Piazza, P.V. (2002). Nicotine self-administration impairs hippocampal plasticity. J. Neurosci. *22*, 3656–3662.

Berg, D.K., and Conroy, W.G. (2002). Nicotinic α7 receptors: synaptic options and downstream signaling in neurons. J. Neurobiol. *53*, 512–523.

Bertrand, S., Weiland, S., Berkovic, S.F., Steinlein, O.K., and Bertrand, D. (1998). Properties of neuronal nicotinic acetylcholine receptor mutants from humans suffering from autosomal dominant nocturnal frontal lobe epilepsy. Br. J. Pharmacol. *125*, 751–760.

Broide, R.S., Salas, R., Ji, D., Paylor, R., Patrick, J.W., Dani, J.A., and De Biasi, M. (2002). Increased sensitivity to nicotine-induced seizures in mice expressing the L250T α7 nicotinic acetylcholine receptor mutation. Mol. Pharmacol. *61*, 695–705.

Buisson, B., and Bertrand, D. (2001). Chronic exposure to nicotine upregulates the human α4β2 nicotinic acetylcholine receptor function. J. Neurosci. *21*, 1819–1829.

Chimienti, F., Hogg, R.C., Plantard, L., Lehmann, C., Brakch, N., Fischer, J., Huber, M., Bertrand, D., and Hohl, D. (2003). Identification of SLURP-1 as an epidermal neuromodulator explains the clinical phenotype of Mal de Meleda. Hum. Mol. Genet. *12*, 3017–3024.

Chorvat, R.J., Zaczek, R., and Brown, B.S. (1998). Ion channel modulators that enhance acetylcholine release: potential therapies for Alzheimer's disease. Expert Opin. Investig. Drugs *7*, 499–518.

Chou, J.H., Bargmann, C.I., and Sengupta, P. (2001). The Caenorhabditis elegans *odr-2* gene encodes a novel Ly-6-related protein required for olfaction. Genetics *157*, 211–224.

Clarke, P.B., and Kumar, T. (1983). The effects of nicotine on locomotor activity in non-tolerant and tolerant rats. Br. J. Pharmacol. *78*, 329–337.

Clarke, G., and Lumsden, C.J. (2005). Heterogeneous cellular environments modulate one-hit neuronal death kinetics. Brain Res. Bull. *65*, 59–67.

Crawley, J.N. (2000). What's Wrong with My Mouse? Behavioral Phenotyping of Transgenic and Knockout Mice (New York: Wiley & Sons, Inc.).

Dajas-Bailador, F.A., Lima, P.A., and Wonnacott, S. (2000). The α7 nicotinic acetylcholine receptor subtype mediates nicotine protection against NMDA excitotoxicity in primary hippocampal cultures through a $Ca^{(2+)}$ dependent mechanism. Neuropharmacology *39*, 2799–2807.

Damaj, M.I., Glassco, W., Dukat, M., and Martin, B.R. (1999). Pharmacological characterization of nicotine-induced seizures in mice. J. Pharmacol. Exp. Ther. *291*, 1284–1291.

Dani, J.A. (2001). Overview of nicotinic receptors and their roles in the central nervous system. Biol. Psychiatry *49*, 166–174.

Dani, J.A., Radcliffe, K.A., and Pidoplichko, V.I. (2000). Variations in desensitization of nicotinic acetylcholine receptors from hippocampus and midbrain dopamine areas. Eur. J. Pharmacol. *393*, 31–38.

Dittman, J.S., Kreitzer, A.C., and Regehr, W.G. (2000). Interplay between facilitation, depression, and residual calcium at three presynaptic terminals. J. Neurosci. *20*, 1374–1385.

Fonck, C., Nashmi, R., Deshpande, P., Damaj, M.I., Marks, M.J., Riedel, A., Schwarz, J., Collins, A.C., Labarca, C., and Lester, H.A. (2003). Increased sensitivity to agonist-induced seizures, straub tail, and hippocampal theta rhythm in knock-in mice carrying hypersensitive α4 nicotinic receptors. J. Neurosci. *23*, 2582–2590.

Fonck, C., Cohen, B.N., Nashmi, R., Whiteaker, P., Wagenaar, D.A., Roderigues-Pinguet, N., Deshpande, P., McKinney, S., Kwoh, S., Munoz, J., et al. (2005). Novel seizure phenotype and sleep disruptions in knock-in mice with hypersensitive α4* nicotinic receptors. J. Neurosci. *25*, 11396–11411.

Fucile, S. (2004). $Ca^{2+}$ permeability of nicotinic acetylcholine receptors. Cell Calcium *35*, 1–8.

Gould, T.J., and Wehner, J.M. (1999). Nicotine enhancement of contextual fear conditioning. Behav. Brain Res. *203*, 31–39.

Hurst, R.S., Hajos, M., Raggenbass, M., Wall, T.M., Higdon, N.R., Lawson, J.A., Rutherford-Root, K.L., Berkenpas, M.B., Hoffmann, W.E., Piotrowski, D.W., et al. (2005). A novel positive allosteric modulator of the α7 neuronal nicotinic acetylcholine receptor: *in vitro* and *in vivo* characterization. J. Neurosci. *25*, 4396–4405.

Ibanez-Tallon, I., Miwa, J.M., Wang, H.L., Adams, N.C., Crabtree, G.W., Sine, S.M., and Heintz, N. (2002). Novel modulation of neuronal nicotinic acetylcholine receptors by association with the endogenous prototoxin lynx1. Neuron *33*, 893–903.

Kaneko, W.M., Britto, L.R.G., Lindstrom, J.M., and Karten, H.J. (1998). Distribution of the α7 nicotinic acetylcholine receptor subunit in the developing chick cerebellum. Brain Res. Dev. Brain Res. *105*, 141–145.

Kelton, M.C., Kahn, H.J., Conrath, C.L., and Newhouse, P.A. (2000). The effects of nicotine on Parkinson's disease. Brain Cogn. *43*, 274–282.

King, S.L., Caldarone, B.J., and Picciotto, M.R. (2004). β2-subunit-containing nicotinic acetylcholine receptors are critical for dopamine-dependent locomotor activation following repeated nicotine administration. Neuropharmacology *47*, 132–139.

Klein, R.C., and Yakel, J.L. (2005). Paired-pulse potentiation of α7-containing nAChRs in rat hippocampal CA1 stratum radiatum interneurones. J. Physiol. *568*, 881–889.

Kuryatov, A., Gerzanich, V., Nelson, M., Olale, F., and Lindstrom, J. (1997). Mutation causing autosomal dominant nocturnal frontal lobe epilepsy alters $Ca^{2+}$ permeability, conductance, and gating of human α4β2 nicotinic acetylcholine receptors. J. Neurosci. *17*, 9035–9047.

Labarca, C., Schwarz, J., Deshpande, P., Schwarz, S., Nowak, M.W., Fonck, C., Nashmi, R., Kofuji, P., Dang, H., Shi, W., et al. (2001). Point mutant mice with hypersensitive α4 nicotinic receptors show dopaminergic deficits and increased anxiety. Proc. Natl. Acad. Sci. USA *98*, 2786–2791.

Lester, H.A., Dibas, M.I., Dahan, D.S., Leite, J.F., and Dougherty, D.A. (2004). Cys-loop receptors: new twists and turns. Trends Neurosci. *27*, 329–336.

Lindstrom, J. (1997). Nicotinic acetylcholine receptors in health and disease. Mol. Neurobiol. *15*, 193–222.

Maelicke, A., Schrattenholz, A., Samochocki, M., Radina, M., and Albuquerque, E.X. (2000). Allosterically potentiating ligands of nicotinic receptors as a treatment strategy for Alzheimer's disease. Behav. Brain Res. *113*, 199–206.

Maggi, L., Sola, E., Minneci, F., Le Magueresse, C., Changeux, J.P., and Cherubini, E. (2004). Persistent decrease in synaptic efficacy induced by nicotine at Schaffer collateral–CA1 synapses in the immature rat hippocampus. J. Physiol. *559*, 863–874.

Mann, E.O., and Greenfield, S.A. (2003). Novel modulatory mechanisms revealed by the sustained application of nicotine in the guinea-pig hippocampus in vitro. J. Physiol. *551*, 539–550.

Mansvelder, H.D., and McGehee, D.S. (2000). Long-term potentiation of excitatory inputs to brain reward areas by nicotine. Neuron *27*, 349–357.

Mansvelder, H.D., Keath, J.R., and McGehee, D.S. (2002). Synaptic mechanisms underlie nicotine-induced excitability of brain reward areas. Neuron *33*, 905–919.

Marks, M.J., Pauly, J.R., Gross, S.D., Deneris, E.S., Hermans-Borgmeyer, I., Heinemann, S.F., and Collins, A.C. (1992). Nicotine binding and nicotinic receptor subunit RNA after chronic nicotine treatment. J. Neurosci. *12*, 2765–2784.

Marks, M.J., Grady, S.R., Yang, J.M., Lippiello, P.M., and Collins, A.C. (1994). Desensitization of nicotine-stimulated $86Rb^{+}$ efflux from mouse brain synaptosomes. J. Neurochem. *63*, 2125–2135.

McGehee, D.S., Heath, M.J., Gelber, S., Devay, P., and Role, L.W. (1995). Nicotine enhancement of fast excitatory synaptic transmission in CNS by presynaptic receptors. Science *269*, 1692–1696.

McLeod, J.R., Shen, M., Kim, D.J., and Thayer, S.A. (1998). Neurotoxicity mediated by aberrant patterns of synaptic activity between rat hippocampal neurons in culture. J. Neurophysiol. *80*, 2688–2698.

Miwa, J.M., Ibanez-Tallon, I., Crabtree, G.W., Sanchez, R., Sali, A., Role, L.W., and Heintz, N. (1999). lynx1, an endogenous toxin-like modulator of nicotinic acetylcholine receptors in the mammalian CNS. Neuron *23*, 105–114.

Orb, S., Wieacker, J., Labarca, C., Fonck, C., Lester, H.A., and Schwarz, J. (2004). Knockin mice with Leu9'Ser α4-nicotinic receptors: substantia nigra dopaminergic neurons are hypersensitive to agonist and lost postnatally. Physiol. Genomics *18*, 299–307.

Orr-Urtreger, A., Broide, R.S., Kasten, M.R., Dang, H., Dani, J.A., Beaudet, A.L., and Patrick, J.W. (2000). Mice homozygous for the L250T mutation in the α7 nicotinic acetylcholine receptor show increased neuronal apoptosis and die within 1 day of birth. J. Neurochem. *74*, 2154–2166.

Pereira, E.F., Hilmas, C., Santos, M.D., Alkondon, M., Maelicke, A., and Albuquerque, E.X. (2002). Unconventional ligands and modulators of nicotinic receptors. J. Neurobiol. *53*, 479–500.

Picciotto, M.R., and Zoli, M. (2002). Nicotinic receptors in aging and dementia. J. Neurobiol. *53*, 641–655.

Picciotto, M.R., Zoli, M., Lena, C., Bessis, A., Lallemand, Y., Le Novere, N., Vincent, P., Pich, E.M., Brulet, P., and Changeux, J.P. (1995). Abnormal avoidance learning in mice lacking functional high-affinity nicotine receptors in the brain. Nature *374*, 65–67.

Picciotto, M.R., Caldarone, B.J., King, S.L., and Zachariou, V. (2000). Nicotinic receptors in the brain. Links between molecular biology and behavior. Neuropsychopharmacology *22*, 451–465.

Quick, M.W., and Lester, R.A. (2002). Desensitization of neuronal nicotinic receptors. J. Neurobiol. *53*, 457–478.

Rathouz, M.M., and Berg, D.K. (1994). Synaptic-type acetylcholine receptors raise intracellular calcium levels in neurons by two mechanisms. J. Neurosci. *11*, 6935–6945.

Rezvani, A.H., and Levin, E.D. (2001). Cognitive effects of nicotine. Biol. Psychiatry *49*, 258–267.

Schafe, G.E., Nader, K., Blair, H.T., and LeDoux, J.E. (2001). Memory consolidation of Pavlovian fear conditioning: a cellular and molecular perspective. Trends Neurosci. *24*, 540–546.

Sekhon, H.S., Song, P., Jia, Y., Lindstrom, J., and Spindel, E.R. (2005). Expression of *lynx1* in developine lung and its modulation by prenatal nicotine exposure. Cell Tissue Res. *320*, 287–297.

Sharma, G., and Vijayaraghavan, S. (2003). Modulation of presynaptic store calcium induces release of glutamate and postsynaptic firing. Neuron *38*, 929–939.

Sheffield, E.B., Quick, M.W., and Lester, R.A. (2000). Nicotinic acetylcholine receptor subunit mRNA expression and channel function in medial habenula neurons. Neuropharmacology *39*, 2591–2603.

Shinnick-Gallagher, P., McKernan, M.G., Xie, J., and Zinebi, F. (2003). L-type voltage-gated calcium channels are involved in the *in vivo* and *in vitro* expression of fear conditioning. Ann. N Y Acad. Sci. *985*, 135–149.

Stevens, T.R., Krueger, S.R., Fitzsimonds, R.M., and Picciotto, M.R. (2003). Neuroprotection by nicotine in mouse primary cortical cultures involves activation of calcineurin and L-type calcium channel inactivation. J. Neurosci. *23*, 10093–10099.

Tapper, A.R., McKinney, S.L., Nashmi, R., Schwarz, J., Deshpande, P., Labarca, C., Whiteaker, P., Marks, M.J., Collins, A.C., and Lester, H.A. (2004). Nicotine activation of $\alpha4^*$ receptors: sufficient for reward, tolerance, and sensitization. Science *306*, 1029–1032.

Trinh, N.H., Hoblyn, J., Mohanty, S., and Yaffe, K. (2003). Efficacy of cholinesterase inhibitors in the treatment of neuropsychiatric symptoms and functional impairment in Alzheimer's disease: a meta-analysis. JAMA *289*, 210–216.

Truong, A., Xing, X., Forsayeth, J.R., Dwoskin, L.P., Crooks, P.A., and Cohen, B.N. (2001). Pharmacological differences between immunoisolated native brain and heterologously expressed rat $\alpha4\beta2$ nicotinic receptors. Brain Res. Mol. Brain Res. *96*, 68–76.

Tsuneki, H., Klink, R., Lena, C., Korn, H., and Changeux, J.P. (2000). Calcium mobilization elicited by two types of nicotinic acetylcholine receptors in mouse substantia nigra pars compacta. Eur. J. Neurosci. *12*, 2475–2485.

US Department of Health and Human Services. (1988). The Health Consequences of Smoking: Nicotine Addiction. A Report of the Surgeon General. U.S. Government Printing Office.

Vijayaraghavan, S., Pugh, P.C., Zhang, Z.W., Rathouz, M.M., and Berg, D.K. (1992). Nicotinic receptors that bind $\alpha$-bungarotoxin on neurons raise intracellular free $Ca^{2+}$. Neuron *8*, 353–362.

Whiteaker, P., Sharples, C.G., and Wonnacott, S. (1998). Agonist-induced up-regulation of $\alpha4\beta2$ nicotinic acetylcholine receptors in M10 cells: pharmacological and spatial definition. Mol. Pharmacol. *53*, 950–962.

Wooltorton, J.R., Pidoplichko, V.I., Broide, R.S., and Dani, J.A. (2003). Differential desensitization and distribution of nicotinic acetylcholine receptor subtypes in midbrain dopamine areas. J. Neurosci. *23*, 3176–3185.

Yu, D., Ellis, H.M., Lee, E.C., Jenkins, N.A., Copeland, N.G., and Court, D.L. (2000). An efficient recombination system for chromosome engineering in Escherichia coli. Proc. Natl. Acad. Sci. USA *97*, 5978–5983.

Zoli, M., Picciotto, M.R., Ferrari, R., Cocchi, D., and Changeux, J.P. (1999). Increased neurodegeneration during ageing in mice lacking high-affinity nicotine receptors. EMBO J. *18*, 1235–1244.